Available online at www.sciencedirect.com
SCIENCE DIRECT®
Journal of Catalysis 227 (2004) 186–201
JOURNAL OF CATALYSIS
www.elsevier.com/locate/jcat

# Effect of site isolation on the preparation and performance of silica-immobilized Ti CGC-inspired ethylene polymerization catalysts

Michael W. McKittrick, Christopher W. Jones *

*School of Chemical & Biomolecular Engineering, Georgia Institute of Technology, 311 Ferst Dr. Atlanta, GA 30332, USA*

Received 5 April 2004; revised 24 June 2004; accepted 26 June 2004

Available online 11 August 2004

**Abstract**

Titanium constrained-geometry-inspired complexes (CGCs) are assembled using several different synthetic protocols on aminosilica scaffolds. In particular, a new synthetic method is reported that utilizes spatially patterned amines on the silica surface to create Ti–CGC sites that are substantially more active for ethylene polymerization than materials prepared using traditional methods. The materials are characterized using multiple techniques including thermogravimetric analysis (TGA), nitrogen physisorption, FT-Raman spectroscopy, $^{29}$Si and $^{13}$C cross-polarization magic-angle spinning (CPMAS) NMR spectroscopy, and diffuse–reflectance UV–visible (UV–vis) spectroscopy. While the new patterning protocol allows for quantitative addition of the cyclopentadienyl group to the surface amines and near quantitative metallation with the titanium source, these steps result in subquantitative additions on aminosilica surfaces prepared via traditional techniques (at high amine loadings) and excess titanium addition (at low amine loadings). Using methylaluminoxane (MAO) as a co-catalyst, the patterned catalyst is more productive than the control materials that were prepared using traditional techniques. However, use of MAO causes significant leaching of the metal complex from the solid support. Using a tris(pentafluorophenyl)borane/trialkylaluminum system as co-catalyst alleviates the leaching problem, allowing for the productivity of the immobilized species to be evaluated. In the polymerization of ethylene, the patterned catalyst is shown to be up to 10 times more productive than the solid control materials. The patterned catalyst is also more active than the homogeneous analogue.


*Keywords:* Constrained-geometry catalyst; Silica surface; Mesoporous silica; Template approach; Olefin polymerization; Leaching

## 1. Introduction

Single-site homogeneous complexes such as constrained-geometry complexes (CGCs) have attracted a great deal of interest in recent years as olefin polymerization catalysts[1] (Scheme 1). These and other soluble single-site transition metal complexes have several advantages over traditional Ziegler–Natta catalysts. In general, single-site catalysts allow for the synthesis of polymers with higher molecular weights and narrower polydispersity indices [1,2]. In addition, by adjusting the symmetry of the complex, polyolefins with controlled tacticity can be produced [3,4]. CGCs are unique in the realm of single-site polymerization catalysts in that the CGC metal center is much less sterically hindered than most other olefin polymerization catalysts [1,2]. As a

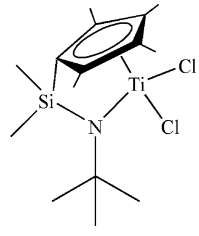


Scheme 1.

* Corresponding author.
*E-mail address:* cjones@chbe.gatech.edu (C.W. Jones).

[1] Group IV CGCs are precatalysts, requiring the addition of a co-catalyst to produce a complex active for olefin polymerization.

0021-9517/$ – see front matter 
doi:10.1016/j.jcat.2004.06.024

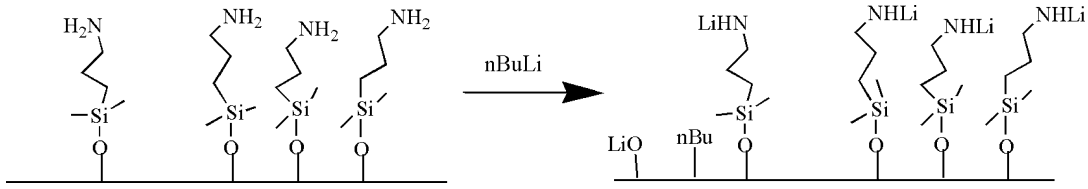


Scheme 2.

result of this accessible reactive site, CGCs have the ability to easily incorporate comonomers, such as 1-hexene or 1-octene, allowing for the synthesis of long-chain or short-chain branches on the polyolefin backbone [1,2].

As a result of these properties, there is considerable interest in constrained-geometry catalysts, as well as metallocenes, a related class of olefin polymerization catalysts. Although these catalysts develop their novel properties from their homogeneous single-site nature, there is a substantial driving force to develop heterogeneous analogues. Most polyolefin plants were developed for use with heterogeneous catalysts (e.g., Ziegler–Natta catalysts, $TiCl_4$ supported on $MgCl_2$; or Phillips catalysts, $Cr_xO_y$ supported on $SiO_2$) in slurry or gas-phase polymerizations [5]. Thus, in many cases, to use a homogeneous catalyst, new plants or significant retrofitting of older plants would be required [6]. Furthermore, when using homogeneous catalysts, reactor fouling is a major concern [6]. Supporting the catalyst on a solid alleviates both of these problems. The most common support used is silica, due to its low cost and ease of functionalization [5].

There are three major ways that metallocenes or other single-site catalysts have been immobilized on silica supports. The first approach, commonly used commercially, is to contact the support material with a co-catalyst (either methyaluminoxane or a combination of a borane and alkylaluminum). The organometallic precatalyst is then added to the support/co-catalyst combination. While this often leads to an effective catalyst, it gives a material that is extremely difficult to characterize and understand on the molecular level, as the activator is typically methylaluminoxane (MAO), an ill-defined oligomeric species [5,7]. In addition, a 100- to 1000-fold excess of aluminum (relative to the transition metal) is routinely used, making molecular characterization of the small number of supported metallocene active sites exceedingly difficult. Thus, to generate a model system that has the potential to be well-characterized on the molecular level, other methods must be developed.

A second method used to support single-site catalysts is to physisorb a complex such as a metallocene or CGC onto the support's surface [8–24]. Alternately, a preformed complex that is designed to form covalent bonds between the ligand and the support could also be used [25–32]. The difficulty with both of these methods stems from the potential reactivity of the preformed complex with the surface silanols [12,22,33]. When a reaction between the silanols on the surface and the metal center occurs, multiple types of sites are often formed, removing the "single-sited" nature of the system.

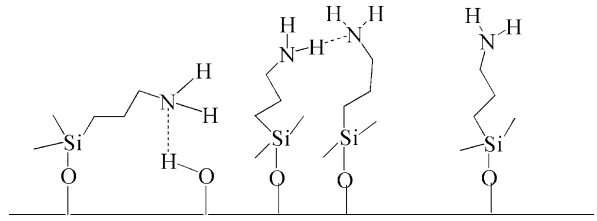


Scheme 3.

A third method is to immobilize the complex via a covalent linkage between the ligand and the support using a multistep grafting approach [34–51]. For instance, cyclopentadienyl ligands have been immobilized on oxide and polymer supports and subsequently metallated to form immobilized metal complexes [52–65]. For immobilizing a CGC, an amine-functionalized support is often used in place of the cyclopentadienyl-functionalized support. Two major difficulties result from this approach if a truly single-site catalyst is desired. First, quite often the procedure used in preparation of the homogeneous complex is simply applied to the supported amine. For example, an alkyl lithium reagent has been used to deprotonate the amines for further functionalization [46–48,66,67]. However, such reagents are extremely harsh toward the silica support and can alkylate the surface, allowing for the formation of multiple types of sites (Scheme 2) [68]. Furthermore, the steric crowding of the amines on the surface as well as interactions between the amines and the surface can create multiple types of anchoring sites (Scheme 3) [69].

Thus, to build a truly single-site CGC on an aminosilica surface via a multistep grafting technique, a well-defined aminosilica (ideally with uniform, isolated sites) is required as a starting material. We have recently reported a patterning protocol (shown in Scheme 4) that allows for the preparation of a well-defined amine-functionalized silica, with amine sites which behave as if they are isolated and uniform [69]. Using this patterned aminosilica as a scaffold, we have subsequently developed a protocol to synthesize a supported titanium constrained-geometry-inspired catalyst on the surface [70]. Here we report the detailed description of the supported patterned CGC[2] and demonstrate its applicability in the catalytic polymerization of ethylene us-

[2] The complexes are referred to as CGCs here, although there is no evidence that the surface complexes prepared in previous works on immobilized CGCs actually have the CGC structure [46–48,70,76]. Although some

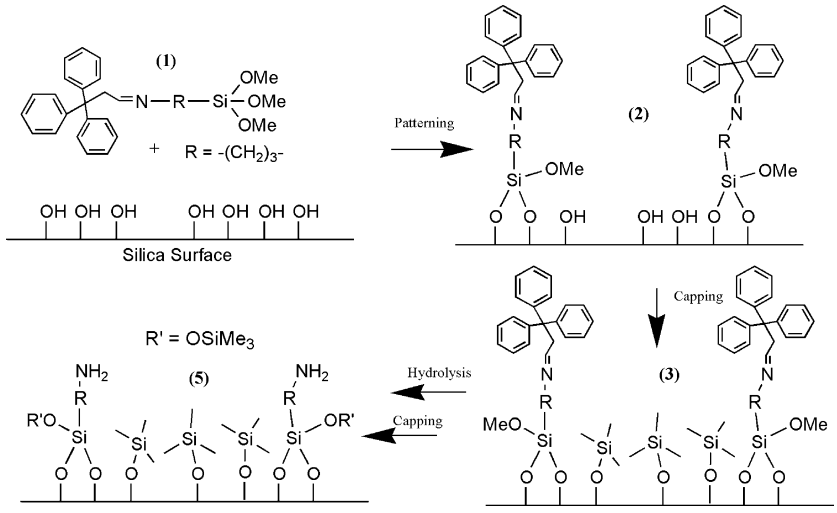


Scheme 4.

ing both methylaluminoxane and borane/trialkylaluminum co-catalysts. In particular, we probe the role of the site isolation on the polymerization performance of the titanium precatalysts and focus on the impact of leaching of the supported metal complexes on the possibility of preparing well-defined, truly single-site model polymerization catalysts using this methodology.

## 2. Experimental

### 2.1. General considerations

The following chemicals were commercially available and used as received: 3,3,3-triphenylpropionic acid (Acros), 1.0 M $LiAlH_4$ in tetrahydrofuran (THF) (Aldrich), pyridinium dichromate (Acros), 2,6-di-*tert*-butylpyridine (Acros), dichlorodimethylsilane (Acros), TEOS (Aldrich), 3-aminopropyltrimethoxysilane (Aldrich), hexamethyldisilazane (Aldrich), tetrakis(diethylamino)titanium (Aldrich), trimethyl silyl chloride (Aldrich), trimethylaluminum (Aldrich), triisobutylaluminum (Aldrich), methylaluminoxane (Aldrich, 10 wt% in toluene), and *n*-butyllithium in hexanes (Aldrich). Tetramethyl-cyclopentadiene (Aldrich) was distilled prior to use. Anhydrous toluene (Acros) was distilled over sodium metal prior to use. Tris(pentafluorophenyl)borane (Aldrich) was purified via sublimation before use. Anhydrous methanol (Acros) was further dried over 4 Å molecular sieves prior to use. Anhydrous ether, anhydrous THF, anhydrous dichloromethane, and anhydrous hexanes were obtained from a packed-bed solvent purification system utilizing columns of copper oxide catalyst and alumina (ether, hexanes) or dual alumina columns (tetrahydrofuran, dichloromethane) [71]. All air- and moisture-sensitive compounds were manipulated using standard vacuum line, Schlenk, or cannula techniques under dry, deoxygenated argon or in a dry box under a deoxygenated nitrogen atmosphere. Ethylene was passed over a metallic catalyst (Matheson 641-01 cartridge) to remove oxygen and water, before being fed to the reactor.

#### 2.1.1. Synthesis of SBA-15

SBA-15 with approximately 50 Å diameter pores was synthesized via literature methods [72,73]. Calcination of the material was done in air using the following temperature program: (1) increasing the temperature (1.2 °C/min) to 200 °C, (2) heating at 200 °C for 1 h, (3) increasing at 1.2 °C/min to 550 °C, and (4) holding at 550 °C for 6 h. Prior to use, the SBA-15 was dried under vacuum at 150 °C for 3 h and stored in a dry box.

#### 2.1.2. Catalyst synthesis

Densely loaded and patterned aminosilica materials were prepared using a SBA-15 host as described previously [69]. From these aminosilica scaffolds, Ti–CGC-inspired complexes were prepared using the methodology previously reported [70].

### 2.2. Synthesis of homogeneous complex ***9***

$Me_4CpSiMe_2Cl$ (1.07 g, 5 mmol) was dissolved in 50 ml of hexane and cooled to −78 °C. To this mixture *n*-propylamine (0.6 g, 10.2 mmol) was added via syringe and the reaction mixture was stirred overnight at and allowed to warm to room temperature. The *n*-propylamine/HCl salt was removed by filtration under argon and the solvent was removed under vacuum yielding the crude product as a yellow oil. Next, 2 mmol of the this crude product $C_5Me_4HSiMe_2NH(CH_2)_2CH_3$ was added via syringe to 2 mmol of $Ti(NEt_2)_4$ dissolved in 20 ml of toluene at −70 °C. The mixture was heated under reflux overnight and the product was obtained as a clear brown oil after

evidence is presented that CGCs are in fact formed in this work, a better term would be “CGC-inspired” complexes as described in the title of this manuscript.

the by-products were removed at 130 °C under high vacuum. The product was then added to a flask with excess chlorotrimethylsilane and hexanes. The reaction was allowed to stir overnight and then the solvent and excess silane were removed under vacuum. NMR ($C_6D_6$): $\delta = 0.21$ (6H, $Si(CH_3)_2$), 1.05 (3H, $CH_2CH_3$), 1.58 (2H, $CH_2CH_2CH_3$), 1.75 (6H, $CpCH_3$), 1.90 (6H, $CpCH_3$), 2.6 (2H, $NCH_2CH_2$). Anal Calc. for $C_{14}H_{21}NCl_2SiTi$, C 48.0%, H 6.0%, N 4.0%, Cl 20.3%, Ti 13.7%. Found C 48.4%, H 5.7%, N 4.6%, Cl 21.5%, Ti 12.9%.

#### 2.2.1. Characterization

FT-Raman spectra were obtained on a Bruker FRA-106. At least 256 scans were collected for each spectrum, with a resolution of 2–4 $cm^{-1}$. Cross-polarization magic-angle spinning (CP-MAS) NMR spectra were collected on a Bruker DSX 300-MHz instrument. Samples were spun in 7-mm zirconia rotors at 5 kHz. The $^{13}C$ CP-MAS parameters were 10000 scans, a 90 pulse length of 4 s, and a delay of 4 s between scans. The $^{29}Si$ CP-MAS parameters were 2000 scans, a 90 pulse length of 5 s, and a delay of 10 s between scans. Nitrogen physisorption measurements were conducted on a Micromeritics ASAP 2010 at 77 K. Samples were pretreated by heating under vacuum at 150 °C for 8 h. Diffuse–reflectance ultraviolet–visible (UV–vis) spectroscopy was performed on solid materials in a dry box with an Ocean Optics USB2000 Fiber Optic Spectrometer using a PTFE diffuse–reflectance standard. Solution UV–vis spectroscopy was performed using a Hewlett Packard Model 8453 spectrometer with anhydrous hexanes as a solvent. Thermogravimetic analysis (TGA) was performed on a Netzsch STA409. Samples were heated under air from 30 to 1000 °C at a rate of 5 °C/min. The organic loading was measured by determining the weight loss from 200 to 650 °C. Elemental analysis was performed by Desert Analytics, Arizona. Gel permeation chromatography was performed at the University of Massachusetts, Amherst, with Polymer Laboratories PL-220 high-temperature GPC equipped with a Wyatt MiniDawn (620 nm diode laser) high-temperature light-scattering detector and refractive index detector at 135 °C using 1,2,4-trichlorobenzene as solvent and calibrated using polystyrene standards. Polyethylene was extracted from silica at 130 °C using TCB as the solvent prior to the GPC analysis.

### 2.3. Ethylene polymerizations

#### 2.3.1. MAO co-catalyst

The immobilized precatalyst was added to the reactor with toluene and methylalumoxane (800 Al:1 Ti) in a dry box. The solution was stirred for 20 min to allow for sufficient activation of the catalyst. The reactor was then sealed and removed from the glove box, placed in a 25 °C water bath, and subsequently connected to an ethylene source at 60 psi. The ethylene was delivered for a prescribed amount of time and the polymerization was terminated by releasing the ethylene pressure and adding acidic ethanol. The precipitated polymers were washed with ethanol and then dried at 70 °C.

#### 2.3.2. Borane co-catalyst

In a typical polymerization, the immobilized precatalyst was added to the reactor with toluene, tris(pentafluorophenyl) borane (1.5 B:1 Ti), and either trimethylaluminum or triisobutylaluminum (400:1 Al:Ti ratio) in a dry box. The mixture was allowed to stir for 30 min to allow for sufficient activation of the catalyst. The reactor was then sealed and removed from the glove box, placed in a 25 °C water bath, and ethylene at 60 psi was introduced as described above. The polymerization was allowed to continue for a prescribed amount of time, and then terminated as noted above. The precipitated polymers were washed with ethanol and then dried at 70 °C.

#### 2.3.3. Leaching experiments

The immobilized precatalyst, toluene, and methylalumoxane (800 Al:1 Ti) were added to a flask in a dry box. The mixture was allowed to stir for 20 min. The mixture was then filtered in the dry box, and the filtrate was added to the reactor with toluene and an additional portion of MAO (200:1 Al:Ti). The reactor was then removed from the glove box, placed in a 25 °C water bath, and contacted ethylene at 60 psi as described above. The polymerization was allowed to continue for a prescribed amount of time and then terminated by adding acidic ethanol. The precipitated polymers were washed with ethanol and then dried at 70 °C.

## 3. Results and discussion

### 3.1. Materials synthesis and characterization

We recently reported a methodology to synthesize an aminosilica material which behaves as if it has uniform, isolated amine functionalities [69]. Scheme 4 shows the patterning protocol developed. Using this unique patterned aminosilica material as a scaffold, potentially site-isolated organometallic catalysts can be prepared [70]. Scheme 5 shows a synthetic protocol that has been developed to prepare immobilized Ti–CGC-inspired species. The first step in the synthesis of the supported complex is the reaction of the supported amine with chlorodimethyl(2,3,4,5-tetramethyl-2,4-cyclopentadien-1-yl)silane (Cp-silane). After contact with two aliquots of the silane, there is quantitative reaction of the silane with the supported amines, as determined by TGA and elemental analysis. When the same procedure is followed using a densely functionalized aminosilica, only two-thirds of the amines react with the silane functionality. This is comparable to results reported in the literature where following treatment with *n*-butyllithium, roughly 70% of the amine groups on a densely functionalized

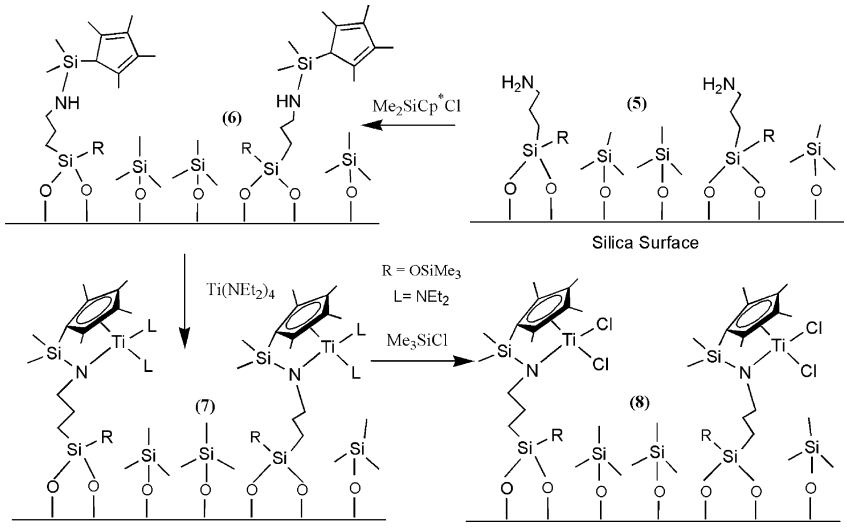


Scheme 5.

surface react with the chlorodimethyl(2,3,4,5-tetramethyl-2,4-cyclopentadien-1-yl)silane [46–48,66,67]. Thus, the ill-defined nature of the densely loaded silica surface results in multiple types of amine sites. In contrast, on the patterned material, the amine sites behave in a more uniform manner. As previously reported, there is no reaction of the chlorodimethyl(2,3,4,5-tetramethyl-2,4-cyclopentadien-1-yl)silane with capped, amine-free SBA-15, as verified again in this work via TGA and UV–vis [69]. In contrast, contacting bare SBA-15 with excess Cp-silane resulted in a pink colored solid, with a loading of 1.07 mmol silane/g solid. These results provide evidence that for reactions on amine-containing solids, the chlorosilane reacts with the amine functionalities on the surface, and does not open siloxane bridges.

A common synthetic route for the preparation of homogeneous metallocenes or CGCs utilizes an alkyl lithium reagent in the next step to deprotonate the Cp ring followed by metallation with the metal tetrachloride salt. However, as noted previously, with silica-supported systems where a single type of site is desired, alkyl lithium reagents must be avoided. Hence, an alternate metallation strategy is required. In this work, after functionalization by the tetramethylcyclopentadienyl silane (Cp′), the support is metallated via an amine elimination method [74,75]. Additional metallation strategies, such as reaction of the ligand with $CpMCl_3$ (Royo method), are also possible [76–79]. Following metallation, the diethylamine ligands on the titanium are exchanged with chlorides, by contacting the complex with trimethylsilyl chloride. Elemental analysis showed essentially quantitative metallation of the amines by the titanium (slightly above 100%, but potentially within experimental error). This compares to ∼50% amine metallation on densely functionalized materials, which is similar to results seen in literature reports [46,55,66,67]. The ligand exchange on the patterned material (**7**) results in nearly quantitative conversion to the chloride form. Elemental analysis shows a chloride loading of 0.72 mmol/g for the patterned material (**8**), resulting in a chlorine to titanium ratio of 1.89 (ideal ratio = 2.0). A chloride loading of 0.95 mmol/g was determined for the densely functionalized material (**12**), which yields a Cl:Ti ratio of 1.81 (ideal ratio = 2.0). These Cl:Ti ratios suggest that the protocol developed (Scheme 5) allows for the titanium metal center to be supported with exchangeable ligands intact. Overall, these elemental analysis results, summarized in Table 1, provide evidence that the use of the novel support with isolated amines leads to a material with more uniform sites than when traditional synthetic techniques are used. However, the potential for side reactions, especially of the titanium source with traces of residual silanols during metallation, cannot be ruled out.

It could be theorized that the incomplete Cp-silane grafting and metallation found on the densely functionalized material is the result of steric constraints on the densely loaded aminosilica, rather than the formation of multiple types of sites with inherently different reactivities. In an attempt to probe this, a low-loading randomly functionalized aminosilica was synthesized by contacting 3-aminopropyltrimethoxysilane with SBA-15, such that 0.46 mmol amine/g solid was supported, giving roughly the same amine loading as the patterned solid. Upon contacting the low-loading randomly functionalized aminosilica with chlorodimethyl(2,3,4,5-tetramethyl-2,4-cyclopentadien-1-yl)silane, 0.32 mmol of silane/g solid was grafted onto the silica surface, which corresponds to 70% of the amine reacting. After metallation with tetrakis(diethylamino)titanium, elemental analysis showed a titanium loading of 0.38 mmol/g solid (material **14**). This corresponds to an amine metallation of 83%, which is higher than material **13** but still less than the quantitative metallation seen in **8**. However, this level of metallation is also equivalent to 119% cyclopentadienyl metallation. This result suggests the formation of multiple types of metal sites on the surface, as the titanium

Table 1
Material functionalization summary

| Material | Patterned silica | Control **11** | Control **12** | Control **13** ("dense") | Control **14** ("random") |
|---|---|---|---|---|---|
| Material description | Patterned silica | Preformed complex on SBA | Stepwise method using *n*-BuLi | Stepwise method without alkyllithiums | Stepwise method without alkyllithiums |
| Amine loading (mmol/g) | 0.35[a,b] | NA | 1.25[a] | 1.25[a] | 0.46[a] |
| Cyclopentadienyl loading (mmol/g) | 0.35[a,b] | NA | 0.84[a,b] | 0.81[a,b] | 0.32[a,b] |
| Ti loading (mmol/g) | 0.38[b] | 0.17[b] | 0.65[b] | 0.53[b] | 0.38[b] |

[a] Determined by TGA.
[b] Determined by EA.

Table 2
$N_2$ physisorption data

| Sample | BET surface area ($m^2$/g-$SiO_2$) | Average pore diameter[a] (Å) |
|---|---|---|
| SBA-15 | 650 | 52 |
| 5 | 589 | 49 |
| 6 | 433 | 44 |
| 7 | 376 | 39 |

[a] Determined from desorption isotherms.

could react with surface silanols, amines on the surface, or immobilized cyclopentadienyl functionalities.

These nonstoichiometric reactions on the densely and randomly loaded materials may be attributed to two potential causes. First, the randomly and densely functionalized solids could indeed have amine sites with different reactivities as hypothesized in our previous report [69]. Or, an alternate cause for this behavior could be the steric constraints imparted by amine sites that exist on the surface in patches even at low loadings [80]. After the first few amine sites in a region react with the Cp-silane moiety, there simply may not be enough room for additional Cp-silane molecules to react with adjacent unreacted amines. Additional studies probing these two hypotheses are underway.

Nitrogen physisorption was used to characterize the silica framework throughout the synthesis. The results are summarized in Table 2. The surface area and average pore diameter decrease upon functionalization of the amine with the cyclopentadienyl functionality, and then decrease again upon metallation with the titanium source. As the mesoporous pore structure is still present, significant pore blockage has not occurred during functionalization. However, the decrease in average pore diameter (from 52 to 39 Å) does show that Ti–CGC-inspired sites were constructed in the pores or along the pore openings.

The materials were also characterized by $^{13}C$ and $^{29}Si$ CP-MAS NMR. Fig. 1 shows the $^{29}Si$ CPMAS NMR spectra of the patterned materials **5**, **6**, and **8**. In each spectra, the resonances for the $Q^2$, $Q^3$, and $Q^4$ silicon resonances can be seen at −92, −100, and −107 ppm, respectively [81].

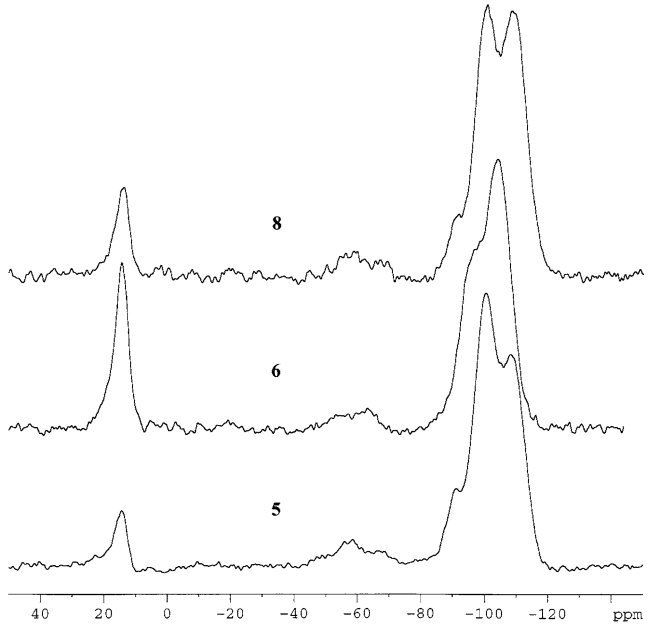


Fig. 1. $^{29}Si$ CP-MAS NMR spectra of patterned aminosilica (**5**), patterned cyclopentadienyl-functionalized SBA-15 (**6**), and metallated Ti–CGC-inspired material (**8**).

The alkyl linkages to the surface can be characterized by the Si–C bond resonances. These resonances, seen at −45, −56, and −67 ppm, correspond to the reaction of 1, 2, and 3 silylmethoxy groups with the surface silanols [82]. The peak at 14 ppm is associated with the Si–C bond found in the capping agent and on the cyclopentadienyl functionality. Although peak heights should not be used to make conclusions since CPMAS NMR is not a quantitative technique, the presence of the signals discussed above suggests the formation of a covalently immobilized surface species.

The $^{13}C$ NMR spectrum in Fig. 2 shows the result of the reaction of the cyclopentadienyl functionality with the patterned aminosilica (**6**). Also illustrated is the spectrum of the metallated solid after ligand exchange (**8**). Specific band assignments are given in Table 3. These NMR spectra show that the expected carbon-containing surface functionalities

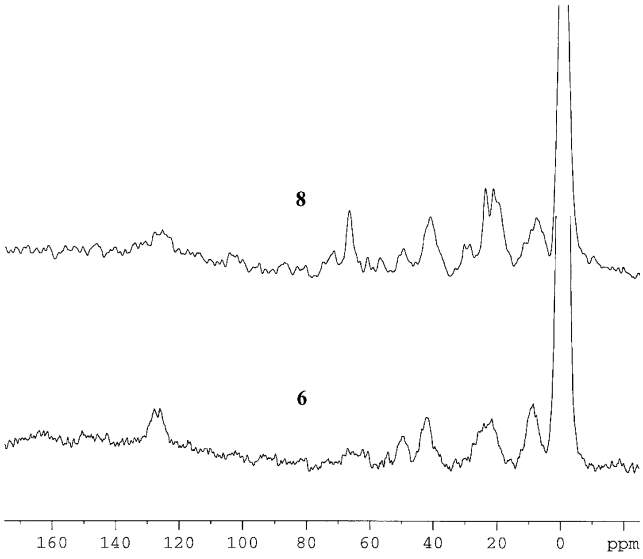


Fig. 2. $^{13}$C CP-MAS NMR spectra of patterned cyclopentadienyl-functionalized SBA-15 (**6**) and metallated Ti–CGC-inspired material (**8**).

Table 3
$^{13}$C CP-MAS assignments for **6** and **8**

| Assignment | Resonance (ppm) |
|---|---|
| Capping agent: –Si–($\mathbf{C}H_3$)$_x$ | 0 |
| Propyl linker: –Si–$\mathbf{C}H_2$–$CH_2$ | 10–14 |
| Cp′ring substituents: ($\mathbf{C}H_3$)$_4$$\mathbf{C}_5$ | |
| Propyl linker: –$CH_2$–$\mathbf{C}H_2$–$CH_2$ | 20–25 |
| Cp′ring substituents: ($\mathbf{C}H_3$)$_4$$\mathbf{C}_5$ | |
| Propyl linker: –N–$\mathbf{C}H_2$–$CH_2$ | 43 |
| Methoxy: –O$\mathbf{C}H_3$ | 50 |
| Cp′ring: ($CH_3$)$_4$$\mathbf{C}_5$ | 128 |

In the spectra, resonance at 67 ppm is a spinning side band of the –Si–($CH_3$)$_x$ resonance.

are present, although even with the use of cross-polarization techniques, the signal to noise ratio is poor. The important resonances present include the carbons in the tetramethylcyclopentadienyl functionality, which can be found at 10–14, 20–25, and 128 ppm. Upon metallation and ligand exchange, little change is expected in the $^{13}$C NMR spectra. Therefore, complementary techniques must be used to further probe the structure of the metallated materials.

Hence, FT-Raman spectroscopy has been also used to characterize the materials. The spectrum of the patterned aminosilica (**5**) is shown in Fig. 3. The large signals at ∼2900 cm$^{-1}$ are associated with aliphatic C–H stretches from the patterned amine and capping agent. The small peak at ∼3050 cm$^{-1}$ corresponds with aromatic C–H stretches due to a small fraction of the trityl imine remaining on the surface. Upon reaction with the cyclopentadienyl silane (material **6**), the signals corresponding to aliphatic carbon–hydrogen vibration (∼2900 cm$^{-1}$) increase as expected. The small amount of aromatic vibrations at 3050 cm$^{-1}$ is still apparent as well. Upon metallation (material **8**), a significant change in the spectra was not expected nor seen, as the organic groups on the surface should not change. The disappearance of some peaks (i.e., the unreacted trityl imine C–H stretches at 3050 cm$^{-1}$) might be attributable to the reactivity of the residual trityl groups with the tetrakis(diethylamino)titanium. Alternately, the loss of these signals may be an artifact of the poorer signal to noise ratio and elevated baseline associated with sample fluorescence of the metallated material. It is noteworthy that the spectrum of the metallated species cannot always be obtained due to fluorescence resulting from the dark orange-brown color of the supported Ti–CGC complex. The combined data from the above techniques are consistent with the presence of the intended surface organic functionalities on the surface. However, as in previous works, little information has been gained concerning the bonding of the transition metal atoms [27,46–48,58,61].

Characterization of the supported complexes is difficult due to the fact that traditional techniques such as NMR, FTIR, and FT-Raman rarely give useful information concerning the bonding of many transition metal centers when the metal species are present at such low concentrations. Hence, in this work, the materials were also characterized by UV–vis spectroscopy in an attempt to elucidate the spe-

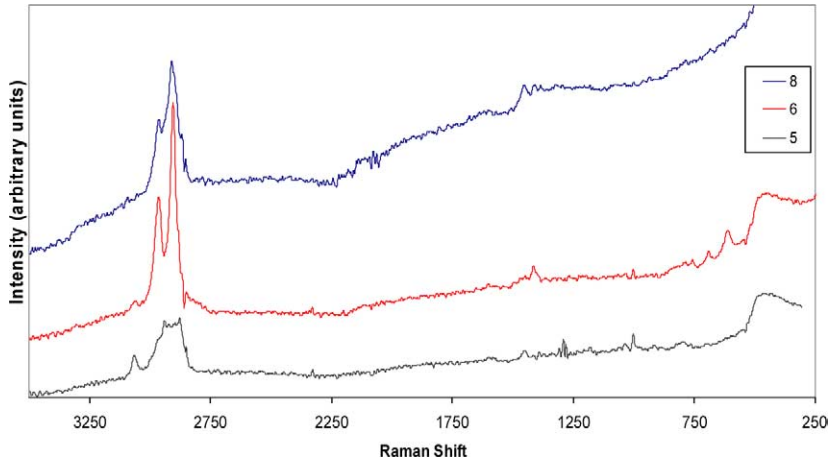


Fig. 3. FT-Raman spectra of patterned aminosilica (**5**), patterned cyclopentadienyl-functionalized SBA-15 (**6**), and metallated Ti–CGC-inspired material (**8**).

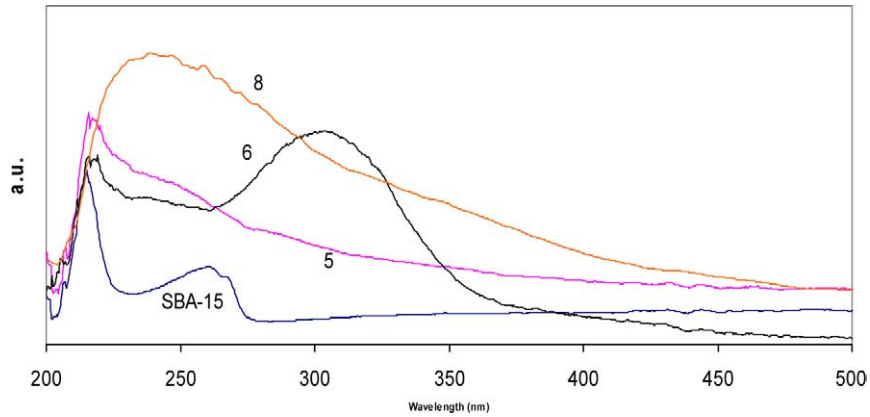


Fig. 4. Diffuse reflectance UV–vis spectra of bare SBA-15, patterned aminosilica (**5**), patterned cyclopentadienyl-functionalized SBA-15 (**6**), and metallated Ti–CGC-inspired material (**8**).

ciation of the metal center (spectra shown in Fig. 4). The UV–vis spectrum for the bare SBA-15 silica has a peak absorbance at 220 nm and a smaller signal at 260 nm. The patterned aminosilica has a broader peak at 220 nm and a shoulder that starts at approximately 240 nm. After reaction of the amines with cyclopentadienyl silane, the spectrum changes further. The peak absorbance seen in material **6** at 310 nm is assigned to a $\pi$ to $\pi^*$ transition of the cyclopentadienyl functionality [83]. Upon metallation to produce material (**8**), the characteristic UV–vis signals change to a peak at 245 nm, likely a transition of the titanium metal center, and a ligand to metal charge transfer (LMCT) signal (from the complexed cyclopentadienyl ligand to the titanium) appearing as a shoulder at 330 nm [83].

To attempt to make more definitive assignments, spectra were obtained for several control materials. Two homogeneous CGC complexes (Scheme 6) were prepared and their UV–vis spectra were obtained. The spectra of the patterned material **8** and homogeneous complexes **9** and **10** are shown in Fig. 5. The homogeneous CGC complex (**9**) has a peak at 260 nm and a shoulder can be seen at about 335 nm. These transitions are similar to the ones seen in material **8**. The

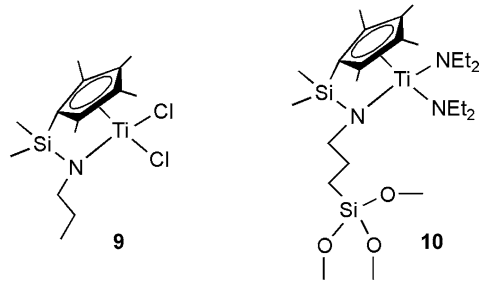


Scheme 6.

homogeneous CGC complex (**10**) has a different spectrum than the other two materials. It has a single broad signal centered at 265 nm, with no the shoulder at 330 nm observed. The transitions at 260 nm for the complexes in the homogeneous solution can be assigned to a transition involving the metal center. The large peak near 200 nm seen in both homogeneous samples is the result of the $\lambda_{end}$ of the solvent, hexanes. In the supported Ti–CGC (**8**), there is a broad signal with a maximum intensity at 245 nm. It is unclear as to the exact structure to which this transition can be assigned.

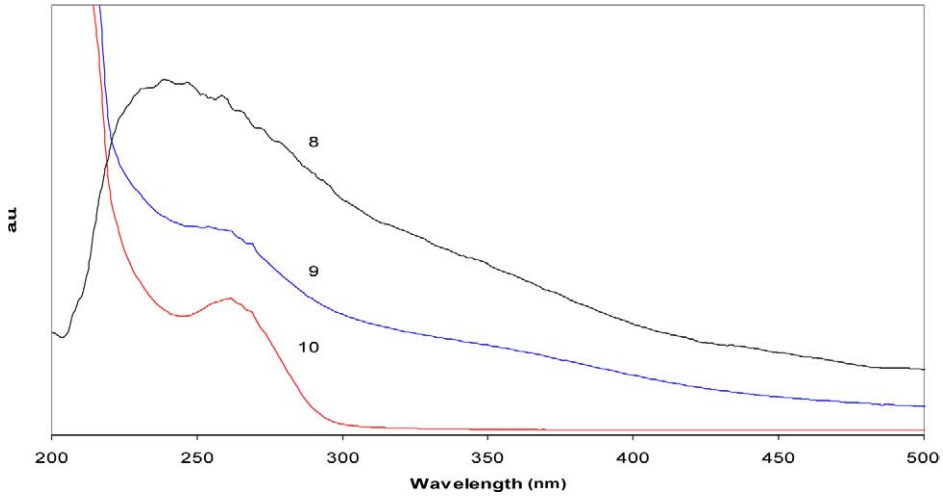


Fig. 5. UV–vis spectra of metallated Ti–CGC-inspired material (**8**), homogeneous CGC complex (**9**), and homogeneous CGC complex (**10**).

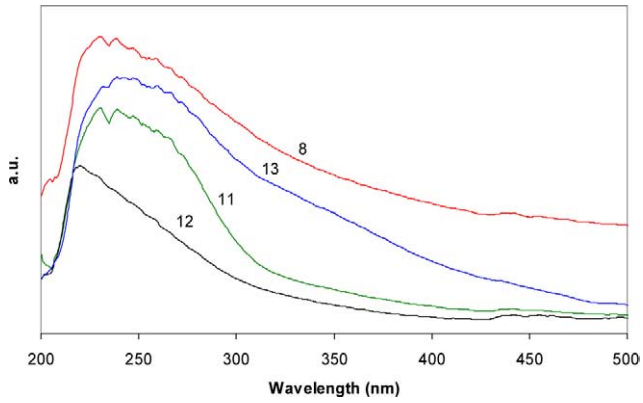


Fig. 6. Diffuse–reflectance UV–vis spectra of metallated Ti–CGC-inspired material (**8**), control material (**11**), control material (**12**), and control material (**13**).

The breadth of the peak could suggest that it may be the amalgamation of the 220 nm signal seen in the silica support (Fig. 4) and the transition from titanium (expected to appear around 260 nm). The homogeneous complex **9** and the patterned material **8** both contain the shoulder at 330 nm, a region where the LMCT from the Cp ring to the Ti is expected to appear. It is noteworthy that this band appears in both samples that contain Ti–Cl ligands (**8**, **9**) but it is absent in the material with Ti–amine ligands (**10**).

Although the similarity between the spectra for the homogeneous control material and the supported complexes is promising, definitive assignments cannot be made until the spectra of several potential structures that could result from side-reactions during the synthesis are examined. In addition, the CGC-inspired materials made via traditional techniques need to be probed.

Fig. 6 shows a comparison of the UV–vis spectra of the patterned material **8** to those of several titanium CGC-inspired control materials. Solid control material **11** was made by supporting the preformed homogeneous complex on silica following Eisen's protocol [27]. Control material **12** was made following Pakkanen's method that utilizes a stepwise grafting approach including *n*-butyllithium in the treatments [46–48]. Finally, the control materials **13** (high loading) and **14** (low loading) were made using the same protocol as shown in Scheme 5, with the exception that a densely or randomly functionalized aminosilica support instead of the patterned aminosilica was used. In all of the metallated materials, there is a broad signal centered around 240 nm. In control material **11**, a material that contains supported Ti–amine species, the transition seen in the homogeneous complex **9** at 330 nm is notably absent. In contrast, in materials **8** and **13**, materials that are chloride exchanged, this band is quite strong. Based on UV–vis analysis, the patterned material **8** and all the control materials **11**, **13**, and **14** appear qualitatively similar to the homogeneous analogue **10**. Only the *n*-butyllithium-treated material, **12**, stands out as distinctly different, with virtually no intensity beyond 300 nm.

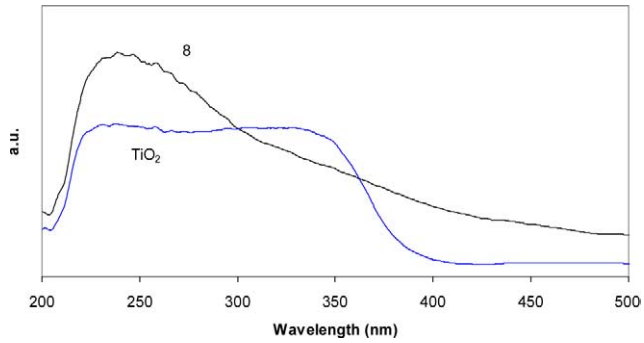


Fig. 7. Diffuse–reflectance UV–vis spectra of metallated Ti–CGC-inspired material (**8**) and titanium dioxide.

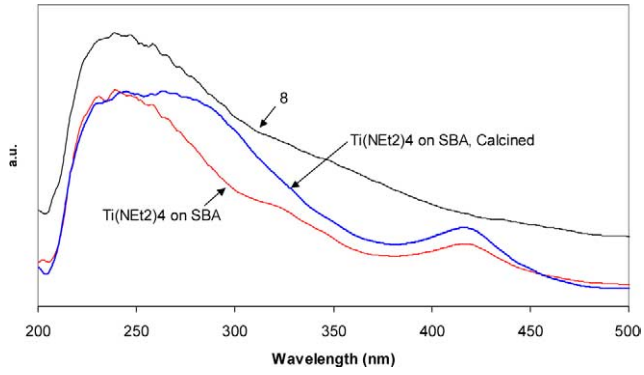


Fig. 8. Diffuse–reflectance UV–vis spectra of metallated Ti–CGC-inspired material (**8**), $Ti(NEt_2)_4$-treated SBA-15, and calcined $Ti(NEt_2)_4$-treated SBA-15.

The supported CGC-inspired complex **8** was also compared to additional titanium-containing materials. One sample was synthesized by contacting tetrakis(diethylamino)-titanium with SBA-15, to give a material that should contain Ti–O–Si linkages [84], species that might be expected if the titanium source reacted with any residual silanols. The UV–vis spectra were taken of this sample before (contains Ti–N and Ti–O linkages) and after (contains only Ti–O linkages) calcinations in air. An additional control material was synthesized by contacting homogeneous complex **9** with bare SBA-15 and capped SBA-15. The final material was titanium dioxide (anatase). The spectrum of $TiO_2$ shows a strong signal at 235 nm, which corresponds to tetrahedrally coordinated titanium, and at 330 nm, which is characteristic of octahedrally coordinated titanium [85]. A comparison of the spectrum of this material with that of **8** can be seen in Fig. 7. The tetrakis(diethylamino)titanium-contacted silica control material has a peak absorption at 240 nm, similar to the transition seen in **8** (Fig. 8). As in the supported CGC case, this broad peak is likely the result of the signal from the silica support and a transition associated with titanium. Additionally, there is a strong signal at 410 nm, possibly the result of the formation of octahedral Ti–O structures [85,86]. There is also a shoulder present around 310 nm. After calcination in air at 100 °C, the signal at 240 nm broadens but is still present as is the peak at

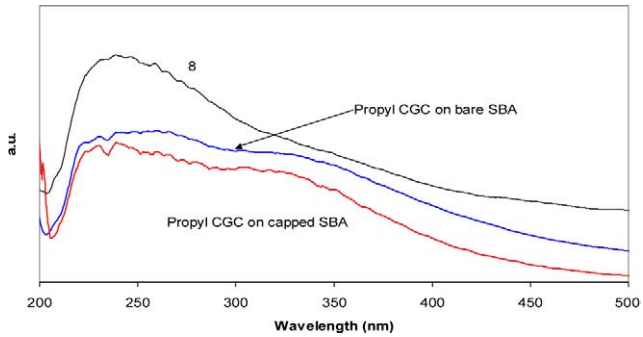


Fig. 9. Diffuse–reflectance UV–vis spectra of metallated Ti–CGC-inspired material (**8**), homogeneous control (**9**) on bare SBA, and homogeneous control (**9**) on capped SBA.

410 nm (shown in Fig. 8). However, the shoulder at 310 nm is less apparent. When the calcination was carried out at 300 °C, the UV–vis spectrum (not shown) is identical to material that was calcined at 100 °C. Overall, the patterned CGC-inspired material appears distinctly different from this control material, especially in the region near 400 nm.

The homogeneous complex **9** was contacted with both bare and capped SBA-15 to try and produce a material with Ti–CGC species but with direct complex–silanol or complex–siloxane bridge interactions. The spectra of the resulting solid can be seen in Fig. 9, along with the spectrum for material **8**. Both materials containing complex **9** and silica have a broad peak spanning from 220 to 260 nm. In addition, a shoulder is present at around 330 nm, as seen in the spectrum of the homogeneous complex **9** in solution. Overall, it is evident that the spectra for both materials are strikingly similar to the CGC-inspired material **8**, providing evidence that the intended CGC structure may have been formed in the patterned material.

While the UV–vis spectrum of the patterned material is consistent with the formation of a constrained-geometry catalyst structure being synthesized on the surface, conclusive assignments of the ligand structure around the titanium based solely on the spectroscopic evidence presented above cannot be made. The transitions associated with the CGC structure are also roughly comparable with many other Ti coordinations with wholly inorganic ligands, for example, titanium dioxide and the material made by contacting tetrakis(diethylamino)titanium with silica followed by calcination. However, these materials show no significant catalytic activity for the polymerization of ethylene. Titanium dioxide only produced trace amounts of polymer and no polymer was formed using the tetrakis(diethylamino)titanium solid. This is in stark contrast to the CGC-inspired materials as noted below.

Through the characterization techniques discussed above, the confirmation of CGC sites cannot be explicitly proven, although the similarity between the UV–vis spectra of **8** and the homogeneous CGC in solution **9** is consistent with the hypothesis that immobilized CGC sites were formed. When these data are combined with the inactivity of supported titanium species with wholly inorganic ligands, it shows that the active Ti species supported via the new protocol developed are very likely ligated by organic ligands. Additional characterization directly probing the metal center is underway.

### 3.2. Ethylene polymerization

The catalytic activity of the materials was evaluated in the polymerization of ethylene. The patterned materials were again compared to the control materials described above: homogeneous analogs **9** and **10** synthesized following literature methods [27]; a solid control material **11** made by supporting the preformed homogeneous complex on silica following Eisen's protocol [27]; control material **12** made following Pakkanen's method that utilizes a stepwise grafting approach including *n*-butyllithium in the treatments [46–48]; and control material **13** was made using the same protocol as shown in Scheme 5, with the exception that a densely functionalized aminosilica support instead of the patterned aminosilica was used. Control **14** is identical to **13** except a randomly functionalized aminosilica with a lower amine loading was used as the scaffold for the CGC. Scheme 7 depicts cartoons of the various supported control materials used in this study.[3] The results of ethylene polymerizations utilizing MAO as a co-catalyst are compiled in Table 4. The patterned catalyst was found to have an activity of 16–20 kg polymer/(mol-Ti h). In comparison to the materials made from densely-loaded aminosilica (**12**, **13**, **14**), the patterned material has an activity that is 4–5 times higher. However, the activity of control **11** was found to be higher than the patterned material. As this material is believed to produce a distribution of sites [27], including some metal–surface interactions, this result was interesting.

In considering these data, it is important to note that MAO is capable of leaching organometallic species from the silica support [29,64,87–89]. To test whether this phenomenon was affecting the precatalysts used in this work, leaching studies were undertaken. The precatalyst was contacted with MAO (800:1 Al:Ti) and toluene in a dry box. The resulting solution was allowed to stir for 20 min, and then the catalyst was removed by filtration. The filtrate was then added to the reactor with an additional portion of MAO. This solution was subsequently exposed to ethylene (60 psig) using the typical polymerization protocol. If the MAO caused leaching of the organometallic complex from the surface, the filtrate should be active in ethylene polymerization. The results of these studies are depicted in Fig. 10.

It is important to note that it is difficult to accurately determine the amount of *active* titanium which leached from the solid. As the leached complexes can be much more active than the supported species, a small fraction of the metal

[3] The cartoons depict hypothesized surface structures for **11**–**14**. There is no direct evidence that these specific titanium sites are formed—they are derived from chemical intuition.

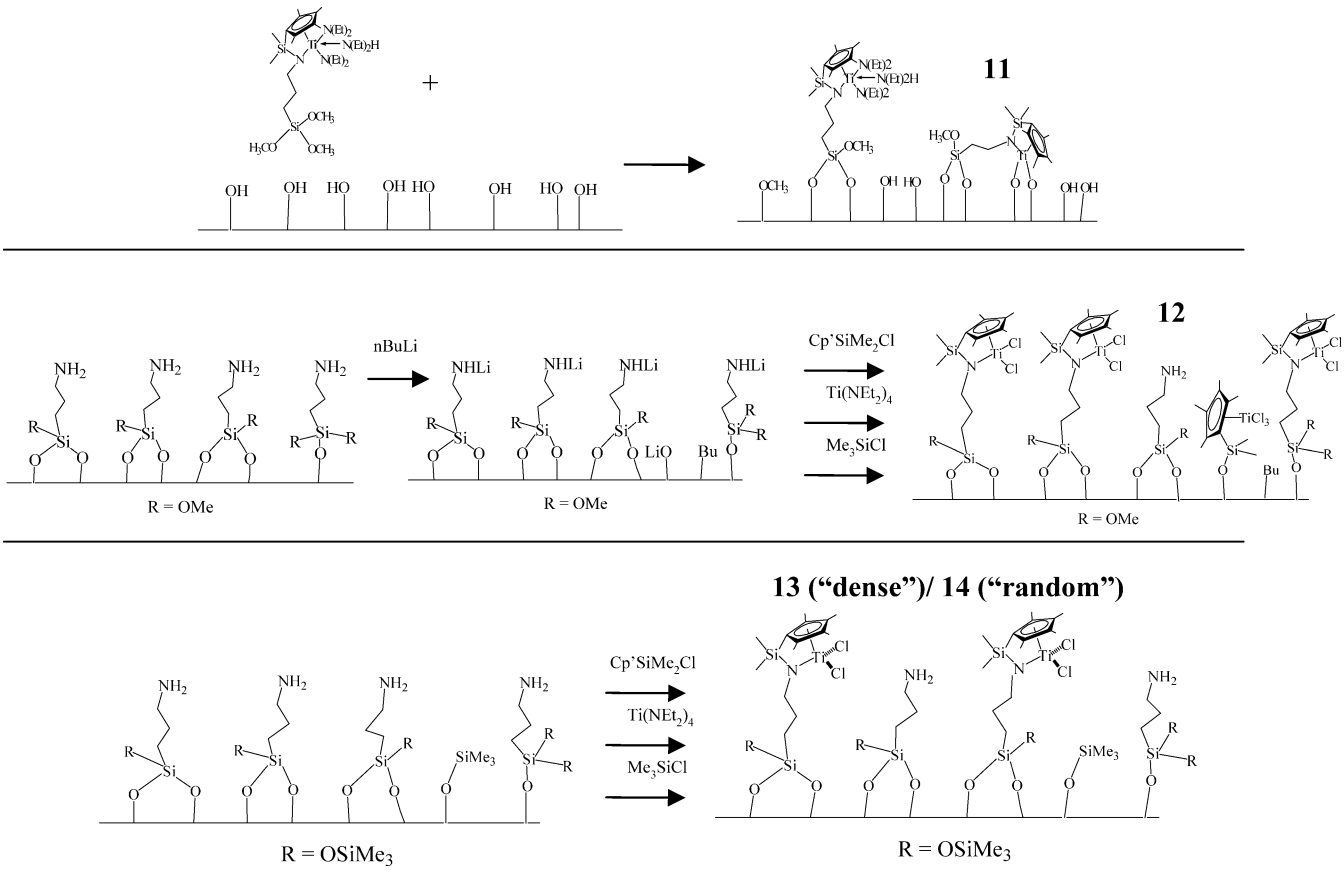


Scheme 7.

Table 4
Ethylene polymerization using MAO as a co-catalyst

| Entry | Catalyst | Ti loading[a] (mmol/$g_{cat}$) | Activation time (min) | Total productivity[b] (kg-PE/(mol-Ti h)) | MW ($\times 10^5$) | PDI |
|---|---|---|---|---|---|---|
| 1 | **8** patterned | 0.38 | 60 | 15.8 | 5.7 | 2.4 |
| 2 | **8** patterned | 0.38 | 20 | 19.7 | 8.9 | 2.3 |
| 3 | **9** control | 2.83 | 20 | 11.4 | – | – |
| 4 | **9** control | 2.83 | 20 | 13.5 | – | – |
| 5 | **10** control | 1.6 | 20 | 6 | – | – |
| 6 | **10** control | 1.6 | 20 | 5.8 | – | – |
| 7 | **11** control | 0.17 | 20 | 26.5 | 7.8 | 2.3 |
| 8 | **12** control | 0.65 | 60 | 4.1 | – | – |
| 9 | **12** control | 0.65 | 20 | 4.2 | – | – |
| 10 | **13** control | 0.53 | 60 | 4.5 | – | – |
| 11 | **13** control | 0.53 | 20 | 5.7 | 4.1 | 4.6 |
| 12 | **13** control | 0.53 | 20 | 5.9 | 2.5 | 5.1 |
| 13 | **14** control | 0.38 | 20 | 5.4 | – | – |

[a] Titanium loadings determined by elemental analysis.
[b] Polymerization conditions: $T = 25\,^{\circ}C$; co-catalyst, MAO; Al/Ti = 800; solvent, toluene; ethylene pressure, 60 psi; reaction time, 10 min.

sites may leach (and an even smaller fraction may actually be active) yet they may provide almost all of the activity observed using the solid catalyst. To determine the amount of leaching from the solid, a nominal activity was calculated based on the total amount of titanium in the solid contacted with the MAO and toluene. By calculating an activity based on the total titanium in a given sample, the percentage of supported activity for a given solid resulting from leaching can be estimated. The results of these experiments should be viewed as a lower bound on the activity of the leached species. The activated species are extremely sensitive, and although all manipulations are performed in a dry box, it is possible there is deactivation through handling.

The patterned catalyst shows that at least 20–30% of its activity is the result of leached species. The control catalyst made via a stepwise approach also shows approximately 20–

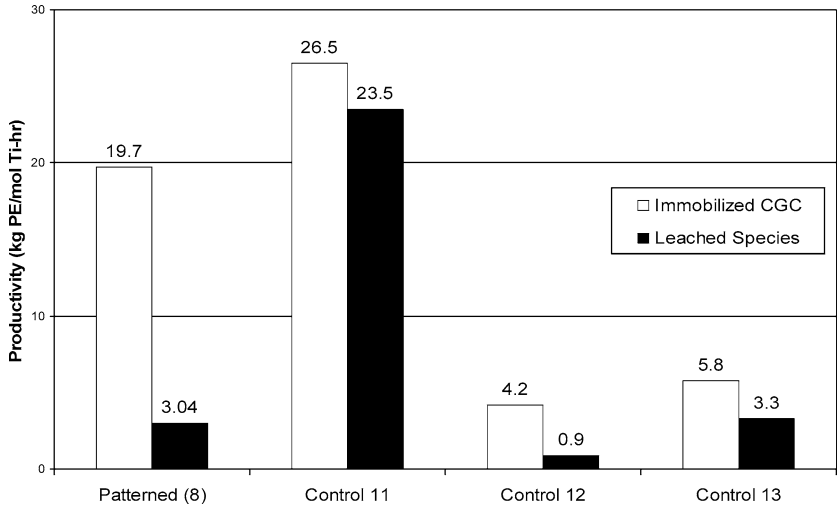


Fig. 10. Comparison of the polyethylene productivity of the supported catalysts with the leached filtrate using methylaluminoxane as a co-catalyst.

30% of its activity resulting from leached species. The other control materials showed that a greater percentage of their activity could be attributed to leaching. Approximately 50% of the activity of the densely functionalized control (**13**) may be attributed to leached species. Almost 90% of the activity of the catalyst made via preformed complex addition (**11**) is attributed to leaching. Thus, this material is more active than the patterned material because highly active, leached Ti species are produced. These results show the significant impact leaching can have on this type of polymerization system. The fact that at least 20% of the activity of the patterned catalyst can be attributed to leached metal complex makes it difficult to make conclusions as to the effect of the patterned scaffold on a supported CGC. Thus, molecular level insight into the supported Ti–CGC-inspired catalysts will likely not be achieved when using MAO as the co-catalyst.

It would be preferable to have a system in which the leaching was negligible or nonexistent. In recent years, it has been shown that an effective class of co-catalysts for metallocenes/constrained-geometry catalysts are borane/alkylaluminum systems [90,91]. In many borane-activated polymerizations, the supported precatalyst is contacted with a molecular borane (i.e., tris[pentafluorylphenyl]borane) and a trialkylaluminum (trimethylaluminum or triisobutylaluminum). An advantage of these types of systems is that the combination of molecular species is more well-defined than the oligomeric MAO activator [92]. Leaching experiments were carried out in a similar manner to those described above. The solid precatalysts were contacted with toluene and trimethylaluminum or triisobutylaluminum in the dry box. After allowing the solution to stir for 30 min, the solid was removed by filtration. The filtrate was then added to the reactor with an aliquot of MAO. This mixture was then exposed to ethylene (60 psig) using the typical polymerization protocol. There was no polymer formed from the filtrate, suggesting that the alkylaluminums do not leach active catalytic sites from the silica. Studies were also undertaken to determine whether the borane/alkylaluminum systems leached inactive titanium species. After contacting the patterned catalyst with trimethylaluminum and toluene as in the leaching studies, the filtrate and solid were analyzed for titanium. No titanium was detectable in solution by elemental analysis, with a resolution of 5 ppm. Additionally, the patterned catalyst was contacted with trimethylaluminum and tris[pentafluorylphenyl]borane, and the solid was removed by filtration. The titanium content of the filtrate was determined by elemental analysis, which again showed no detectable titanium present. This suggests that using the borane/trialkylaluminum co-catalyst systems will allow for the productivity of the immobilized species to be more accurately evaluated.

Fig. 11 depicts the results of the polymerizations utilizing TMA and TIBA in conjunction with tris[pentafluorylphenyl]borane as an activator. The same data are tabulated in Table 5 along with physical properties of the polymers produced. Given that this co-catalyst system does not cause detectable leaching of active species, catalytic results with this system are likely attributable to immobilized catalysts.

Using the borane/trialkylaluminum systems, the patterned system was observed to be significantly more active than the control materials, including the two homogeneous controls **9** and **10**. This mirrors the results seen in the MAO study. The results also give insight into the unexpectedly high activity of **11** using MAO as co-catalyst—most of this activity is attributable to leached species. As the alkylaluminums do not leach the metal complex from the surface, the activity of **11** is greatly decreased compared to the MAO polymerizations. In fact, the activity of the patterned material appears to be slightly enhanced when using a borane co-catalyst. Indeed, there is ample precedence in the literature for activities to be significantly influenced by the nature of the co-catalyst [93,94].

The combination of characterization and polymerization studies show that using a patterned aminosilica as a scaffold for the preparation of a CGC-inspired complex allows for a material which is significantly more active than cat-

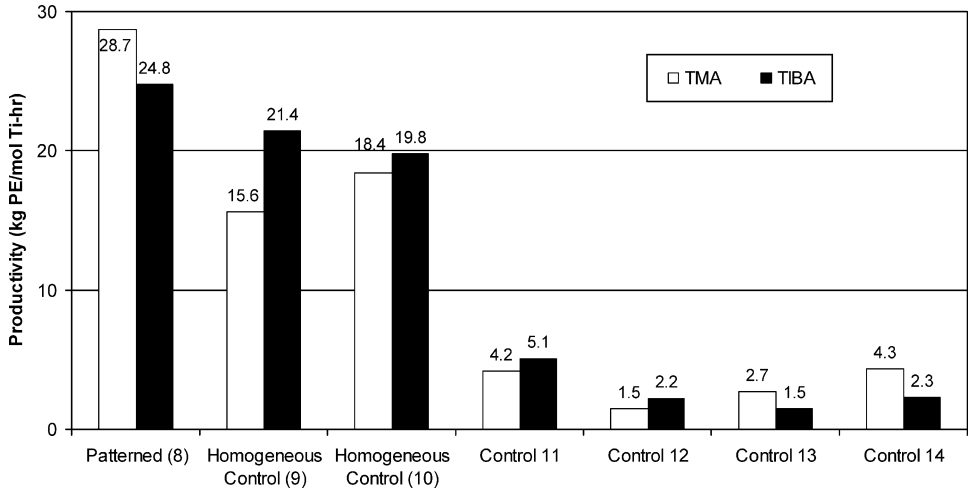


Fig. 11. Polyethylene productivity of the precatalysts using tris(pentafluorophenyl)borane and trimethylaluminum or triethylaluminum as a co-catalyst.

Table 5
Ethylene polymerization using borane/alkylaluminum co-catalysts

| Entry | Catalyst | Ti loading[a] (mmol/$g_{cat}$) | Alkyl aluminum | Productivity[d] (kg-PE/(mol-Ti h)) | $T_m$ (°C) | $M_w$ (polymer) | PDI |
|---|---|---|---|---|---|---|---|
| 1 | **8** patterned | 0.38 | TMA[b] | 28.7 | 134.1 | 660,000 | 3.1 |
| 2 | **8** patterned | 0.38 | TIBA[c] | 24.8 | 133.8 | 1,000,000 | 1.9 |
| 3 | **9** control | 2.83 | TMA | 15.6 | – | – | – |
| 4 | **9** control | 2.83 | TIBA | 21.4 | – | – | – |
| 5 | **10** control | 1.6 | TMA | 18.4 | 133.9 | – | – |
| 6 | **10** control | 1.6 | TIBA | 19.8 | 132.8 | 470,000 | 2.8 |
| 7 | **11** control | 0.17 | TMA | 4.2 | 131.5 | – | – |
| 8 | **11** control | 0.17 | TIBA | 5.1 | 132.6 | 620,000 | 2.5 |
| 9 | **12** control | 0.65 | TMA | 1.5 | 131.9 | – | – |
| 10 | **12** control | 0.65 | TIBA | 2.2 | 133.2 | – | – |
| 11 | **13** control | 0.53 | TMA | 2.7 | 133.5 | 500,000 | Broad |
| 12 | **13** control | 0.53 | TIBA | 1.5 | 133.1 | 1,000,000 | 2 |
| 13 | **14** control | 0.38 | TMA | 4.3 | – | – | – |
| 14 | **14** control | 0.38 | TIBA | 2.3 | – | – | – |

[a] Titanium loadings determined by elemental analysis.
[b] TMA, trimethylaluminum.
[c] TIBA, triisobutylaluminum.
[d] Polymerization conditions: $T = 25°C$; co-catalyst, tris(pentafluorophenyl)borane; Al/Ti = 400; solvent, toluene; ethylene pressure, 60 psi; reaction time, 10 min.

alysts assembled on densely functionalized materials. The patterned silica allows for sites which may be uniform and isolated to be synthesized, although the exact mechanism for the increased reactivity is not yet certain. One possible explanation is that the patterning protocol produces a metal center that cannot interact with free amines on the surface, as the data suggest essentially all of the amines are functionalized, in contrast to the densely and randomly functionalized materials (**12**–**14**). To elucidate the impact of excess amines, the catalytic productivity of the materials with free amines in solution was determined. The catalysts were activated as discussed above, using both MAO and borane/alkylaluminum systems. After activation of the catalyst, propyl amine (200:1 N:Ti) was added to the mixture, which was then exposed to ethylene as previously described. The results are summarized in Table 6. In comparison to the catalytic results shown in Tables 4 and 5, adding free amine to the polymerization caused a significant decrease in the productivity of the catalysts. As the free amines can ligate to the metal center, it is possible that the open site on the titanium necessary for monomer coordination is filled by the propyl amine. While the presence of the co-catalyst in the polymerization can continue to create the necessary active species, the amine is shown to reduce the efficiency of this process. These results may suggest an explanation for the decreased activity of the densely functionalized materials compared to the patterned catalysts. It is possible that the supported metal centers interact with amines in close proximity on the surface, forming a less active catalytic site. Indeed, in another work, we have recently shown that complexes that are formed through interaction of Zr with Cp and amine groups that are not directly linked are substantially less active than catalysts that

Table 6
Ethylene polymerization with added free amine

| Entry | Catalyst | Ti loading[a] ($mmol/g_{cat}$) | Cocatalyst | Amine equivalents | Productivity[e] (kg-PE/(mol-Ti h)) |
|---|---|---|---|---|---|
| 1 | **8** patterned | 0.38 | Borane[b]/TMA[c] | 200 | 6.3 |
| 2 | **8** patterned | 0.38 | Borane[b]/TMA[d] | 200 | 6.9 |
| 3 | **8** patterned | 0.38 | MAO | 200 | 5.1 |
| 4 | **9** control | 2.83 | Borane[b]/TMA[c] | 200 | 0.5 |
| 5 | **9** control | 2.83 | Borane[b]/TMA[d] | 200 | Trace |
| 6 | **9** control | 2.83 | MAO | 200 | Trace |
| 7 | **13** control | 0.53 | Borane[b]/TMA[c] | 200 | 1.0 |
| 8 | **13** control | 0.53 | Borane[b]/TMA[d] | 200 | Trace |
| 9 | **13** control | 0.53 | MAO | 200 | 0.7 |
| 7 | **14** control | 0.38 | Borane[b]/TMA[c] | 200 | 1.6 |
| 8 | **14** control | 0.38 | Borane[b]/TMA[d] | 200 | 2.4 |
| 9 | **14** control | 0.38 | MAO | 200 | 1.1 |

[a] Titanium loadings determined by elemental analysis.
[b] Borane, tris(pentafluorophenyl)borane.
[c] TMA, trimethylaluminum.
[d] TIBA, triisobutylaluminum.
[e] Polymerization conditions: $T = 25°C$; solvent, toluene; ethylene pressure, 60 psi; reaction time, 10 min.

have the true CGC structure [79]. However, it is highly unlikely that this can completely explain the decreased rates over the nonpatterned catalysts. It is noteworthy that 200 eq of added amine reduced the activity of **8** by 80%. However, this reduced activity was still 50–150% higher than the densely loaded material in the absence of added amine. As the dense material has roughly 0.5 eq of extra surface amines (compared 200× excess in the homogeneous case described above) and the amines are not as mobile as the homogeneous amines, it is clear that the additional amine cannot account for all or even most of the observed activity difference.

It is noteworthy that the patterned material **8** is found be unique in two aspects—the quantitative nature of the complex synthesis on the surface (e.g., metallation efficiency of ∼ 1 Ti:N) and its catalytic productivity. This supports the hypothesis that preparation of accessible, potentially more uniform surface species is the likely cause of the observed elevated productivity (in lieu of the preparation of different, more active species on the patterned aminosilica).[4] The isolation could improve polymerization activity by allowing for more efficient and complete activation of the metal center. It could also allow for faster diffusion of the monomer to the reactive center. At this point, it is difficult to determine whether the spatial patterning, removal of surface silanols through capping, or some combination of the two make the patterned precatalyst a more active species than the control materials. Work is currently underway to help shed light on this issue.

It should be noted that there are limitations associated with the polymerization reactor used in the work reported here. The activity was determined by collecting the polymer produced in the reactor and averaging this productivity over the time of monomer exposure. Through this method, it is impossible to determine the initial activity, deactivation rates, or steady-state productivity of the catalysts. It is desirable to be able to monitor the activity of the catalyst throughout the duration of the polymerization. This will allow for better conclusions to be drawn regarding the performance of the patterned catalyst versus the control materials. Experiments along these lines are underway.

[4] Utilizing the patterned aminosilica support in conjunction with a different metallation strategy, the evidence supports the formation of different, more active transition metal species on the silica surface [79].

## 4. Conclusions

An immobilized Ti constrained-geometry-inspired catalyst was prepared using a well-defined, site-isolated aminosilica. In using this patterned aminosilica, the synthesis of well-defined, single-sited immobilized Ti–CGC species was desired. The functionalization of the patterned silica proceeded at practically quantitative conversion, unlike when traditionally prepared aminosilica materials were used as scaffolds. The synthesis of the supported complexes was evaluated at each stage by multiple techniques. The compilation of data is consistent with the formation of the desired species on the silica surface, although definitive proof of sites with the CGC structure could not be obtained. While UV–vis spectroscopy provided evidence that the immobilized metallated species could have the CGC structure, conclusive assignment of the titanium bonding could not be made due to similarities of the spectra of the CGC-inspired materials and the control materials. Indeed, it appears that UV–vis spectroscopy, while helpful, may not be the best probe for elucidating the titanium bonding in these systems.

The ethylene polymerization productivity of the patterned catalyst was compared to control materials made by literature protocols. Using MAO as a co-catalyst, the patterned material was significantly more productive than most of the control materials. However, these results are skewed by the leaching phenomenon caused by interaction of the MAO with the supported materials. As such, this yields an ambiguous system, making analysis of the immobilized species difficult. To truly compare the supported materials, a borane/alkylaluminum co-catalyst system was used, which did not cause detectable leaching in the catalysts studied. Using tris(pentafluorophenyl)borane, along with either trimethylaluminum or triisobutylaluminum, it was found that the patterned materials have a productivity of 5–10 times that of any solid supported control material evaluated here.

These polymerization results, when combined with the synthesis and characterization data, suggest that the patterned aminosilica scaffold yields a polymerization catalyst which behaves as if its sites are more accessible and uniform than those resulting from literature protocols. This relatively well-defined system is a good candidate for future structural studies.

## Acknowledgments

C.W.J. thanks the NSF for support through the CAREER program (CTS-0133209). M.W.M. thanks the GT Molecular Design Institute (under prime contract N00014-95-1-1116 from the Office of Naval Research) for partial support through a graduate fellowship. We thank the Coughlin group at UMass for GPC analysis.

## References

[1] A.L. McKnight, R.M. Waymouth, Chem. Rev. 98 (1998) 2587.
[2] G.J.P. Britovsek, V.C. Gibson, D.F. Wass, Angew Chem. Int. Ed. 38 (1999) 428.
[3] A.L. McKnight, M.A. Masood, R.M. Waymouth, D.A. Straus, Organometallics 16 (1997) 2879.
[4] G.W. Coates, Chem. Rev. 100 (2000) 1223.
[5] G.G. Hlatky, Chem. Rev. 100 (2000) 1347.
[6] T.Y. Xie, K.B. McAuley, J.C.C. Hsu, D.W. Bacon, Ind. Eng. Chem. Res. 33 (1994) 449.
[7] J.N. Pedeutour, K. Radhakrishnan, H. Cramail, A. Deffieux, Macromol. Rapid Commun. 22 (2001) 1095.
[8] K. Soga, J.R. Park, T. Shiono, Polym. Commun. 32 (1991) 310.
[9] K. Soga, T. Shiono, H.J. Kim, Makromol. Chem. 194 (1993) 3499.
[10] W. Kaminsky, F. Renner, Makromol. Chem. Rapid Commun. 14 (1993) 239.
[11] N.V. Semikolenova, V.A. Zakharov, Macromol. Chem. Phys. 198 (1997) 2889.
[12] N.G. Dufrenne, J.P. Blitz, C.C. Meverden, Microchem. J. 55 (1997) 192.
[13] R. Quijada, R. Rojas, L. Alzamora, J. Retuert, F.M. Rabagliati, Catal. Lett. 46 (1997) 107.
[14] J. Dupuy, R. Spitz, J. Appl. Polym. Sci. 65 (1997) 2281.
[15] J.T. Xu, J. Zhao, Z.Q. Fan, L.X. Feng, Macromol. Rapid Commun. 18 (1997) 875.
[16] S.B. Roscoe, J.M.J. Frechet, J.F. Walzer, A.J. Dias, Science 280 (1998) 270.
[17] B.L. Moroz, N.V. Semikolenova, A.V. Nosov, V.A. Zakharov, S. Nagy, N.J. O'Reilly, J. Mol. Catal. A 130 (1998) 121.
[18] J.H.Z. dos Santos, M.B. da Rosa, C. Krug, F.C. Stedile, M.C. Haag, J. Dupont, M.D. Forte, J. Polym. Sci. Polym. Chem. 37 (1999) 1987.
[19] J.H.Z. dos Santos, A. Larentis, M.B. da Rosa, C. Krug, I.J.B. Baumvol, J. Dupont, F.C. Stedile, M.D. Forte, Macromol. Chem. Phys. 200 (1999) 751.
[20] J.H.Z. dos Santos, C. Krug, M.B. da Rosa, F.C. Stedile, J. Dupont, M.D. Forte, J. Mol. Catal. A 139 (1999) 199.
[21] S.B. Roscoe, C.G. Gong, J.M.J. Frechet, J.F. Walzer, J. Polym. Sci. Polym. Chem. 38 (2000) 2979.
[22] M. Jezequel, V. Dufaud, M.J. Ruiz-Garcia, F. Carrillo-Hermosilla, U. Neugebauer, G.P. Niccolai, F. Lefebvre, F. Bayard, J. Corker, S. Fiddy, J. Evans, J.P. Broyer, J. Malinge, J.M. Basset, J. Am. Chem. Soc. 123 (2001) 3520.
[23] K. Musikabhumma, T.P. Spaniol, J. Okuda, J. Polym. Sci. Polym. Chem. 41 (2003) 528.
[24] M.C. Sacchi, D. Zucchi, I. Tritto, P. Locatelli, T. Dallocco, Macromol. Rapid Commun. 16 (1995) 581.
[25] D.H. Lee, K.B. Yoon, S.K. Noh, Macromol. Rapid Commun. 18 (1997) 427.
[26] M.C.W. Chan, K.C. Chew, C.I. Dalby, V.C. Gibson, A. Kohlmann, I.R. Little, W. Reed, Chem. Commun. (1998) 1673.
[27] M. Galan-Fereres, T. Koch, E. Hey-Hawkins, M.S. Eisen, J. Organomet. Chem. 580 (1999) 145.
[28] N. Suzuki, H. Asami, T. Nakamura, T. Huhn, A. Fukuoka, M. Ichikawa, M. Saburi, Y. Wakatsuki, Chem. Lett. (1999) 341.
[29] B.Y. Lee, J.S. Oh, Macromolecules 33 (2000) 3194.
[30] J. Tian, Y. Soo-Ko, R. Metcalfe, Y.D. Feng, S. Collins, Macromolecules 34 (2001) 3120.
[31] N. Suzuki, J. Yu, N. Shioda, H. Asami, T. Nakamura, T. Huhn, A. Fukuoka, M. Ichikawa, M. Saburi, Y. Wakatsuki, Appl. Catal. A 224 (2002) 63.
[32] Y.H. Zhang, L.R. Sita, Chem. Commun. (2003) 2358.
[33] P.J. Toscano, T.J. Marks, Langmuir 2 (1986) 820.
[34] K. Soga, H.J. Kim, T. Shiono, Macromol. Chem. Phys. 195 (1994) 3347.
[35] K. Soga, H.J. Kim, T. Shiono, Macromol. Rapid Commun. 15 (1994) 139.
[36] K. Soga, Macromol. Symp. 89 (1995) 249.
[37] K. Soga, T. Arai, B.T. Hoang, T. Uozumi, Macromol. Rapid Commun. 16 (1995) 905.
[38] J.H. Jin, T. Uozumi, K. Soga, Macromol. Rapid Commun. 16 (1995) 317.
[39] K. Soga, H.T. Ban, T. Arai, T. Uozumi, Macromol. Chem. Phys. 198 (1997) 2779.
[40] T. Arai, H.T. Ban, T. Uozumi, K. Soga, Macromol. Chem. Phys. 198 (1997) 229.
[41] S.C. Hong, H.T. Ban, N. Kishi, J.Z. Jin, T. Uozumi, K. Soga, Macromol. Chem. Phys. 199 (1998) 1393.
[42] S.C. Hong, T. Teranishi, K. Soga, Polymer 39 (1998) 7153.
[43] T. Arai, H.T. Ban, T. Uozumi, K. Soga, J. Polym. Sci. Polym. Chem. 36 (1998) 421.
[44] D.H. Lee, H.B. Lee, S.K. Noh, B.K. Song, S.M. Hong, J. Appl. Polym. Sci. 71 (1999) 1071.
[45] H.T. Ban, T. Uozumi, T. Sano, K. Soga, Macromol. Chem. Phys. 200 (1999) 1897.
[46] H. Juvaste, T.T. Pakkanen, E.I. Iiskola, Organometallics 19 (2000) 4834.
[47] H. Juvaste, T.T. Pakkanen, E.I. Iiskola, Organometallics 19 (2000) 1729.
[48] H. Juvaste, T.T. Pakkanen, E.I. Iiskola, J. Organomet Chem. 606 (2000) 169.
[49] H. Schneider, G.T. Puchta, F.A.R. Kaul, G. Raudaschl-Sieber, F. Lefebvre, G. Saggio, D. Mihalios, W.A. Herrmann, J.M. Basset, J. Mol. Catal. A 170 (2001) 127.
[50] N. Medard, J.C. Soutif, I. Lado, C. Esteyries, F. Poncin-Epaillard, Macromol. Chem. Phys. 202 (2001) 3606.
[51] H.G. Alt, P. Schertl, A. Koppl, J. Organomet Chem. 568 (1998) 263.
[52] R.H. Grubbs, C. Gibbons, L.C. Kroll, W.D. Bonds, C.H. Brubaker, J. Am. Chem. Soc. 95 (1973) 2373.
[53] W.D. Bonds, C.H. Brubaker, E.S. Chandrasekaran, C. Gibbons, R.H. Grubbs, L.C. Kroll, J. Am. Chem. Soc. 97 (1975) 2128.
[54] A. Reissova, Z. Bastl, M. Capka, Collect Czech Chem. C 51 (1986) 1430.
[55] E.I. Iiskola, S. Timonen, T.T. Pakkanen, O. Harkki, P. Lehmus, J.V. Seppala, Macromolecules 30 (1997) 2853.
[56] T. Kitagawa, T. Uozumi, K. Soga, T. Takata, Polymer 38 (1997) 615.
[57] A.G.M. Barrett, Y.R. de Miguel, Chem. Commun. (1998) 2079.
[58] S. Timonen, T.T. Pakkanen, E.I. Iiskola, J. Organomet. Chem. 582 (1999) 273.
[59] M. Stork, M. Koch, M. Klapper, K. Mullen, H. Gregorius, U. Rief, Macromol. Rapid Commun. 20 (1999) 210.
[60] H.G. Alt, J. Chem. Soc. Dalton Trans. (1999) 1703.
[61] S. Timonen, T.T. Pakkanen, E.I. Iiskola, J. Mol. Catal. A 148 (1999) 235.
[62] A.M. Uusitalo, T.T. Pakkanen, E.I. Iiskola, J. Mol. Catal. A 156 (2000) 181.
[63] M. Koch, M. Stork, M. Klapper, K. Mullen, H. Gregorius, Macromolecules 33 (2000) 7713.
[64] A.M. Uusitalo, T.T. Pakkanen, E.I. Iskola, J. Mol. Catal. A 177 (2002) 179.
[65] A.G.M. Barrett, Y.R. de Miguel, Tetrahedron 58 (2002) 3785.
[66] H. Juvaste, E.I. Iiskola, T.T. Pakkanen, J. Organomet. Chem. 587 (1999) 38.

[67] H. Juvaste, E.I. Iiskola, T.T. Pakkanen, J. Mol. Catal. A 150 (1999) 1.
[68] T. Tao, G.E. Maciel, J. Am. Chem. Soc. 122 (2000) 3118.
[69] M.W. McKittrick, C.W. Jones, Chem. Mater. 15 (2003) 1132.
[70] M.W. McKittrick, C.W. Jones, J. Am. Chem. Soc. 126 (2004) 3052.
[71] A.B. Pangborn, M.A. Giardello, R.H. Grubbs, R.K. Rosen, F.J. Timmers, Organometallics 15 (1996) 1518.
[72] D.Y. Zhao, J.L. Feng, Q.S. Huo, N. Melosh, G.H. Fredrickson, B.F. Chmelka, G.D. Stucky, Science 279 (1998) 548.
[73] D.Y. Zhao, Q.S. Huo, J.L. Feng, B.F. Chmelka, G.D. Stucky, J. Am. Chem. Soc. 120 (1998) 6024.
[74] G.M. Diamond, R.F. Jordan, J.L. Petersen, J. Am. Chem. Soc. 118 (1996) 8024.
[75] D.W. Carpenetti, L. Kloppenburg, J.T. Kupec, J.L. Petersen, Organometallics 15 (1996) 1572.
[76] R.M. Kasi, E.B. Coughlin, Organometallics 22 (2003) 1534.
[77] S. Ciruelos, T. Cuenca, R. Gomez, P. GomezSal, A. Manzanero, P. Royo, Organometallics 15 (1996) 5577.
[78] B. Royo, P. Royo, L.M. Cadenas, J. Organomet. Chem. 551 (1998) 293.
[79] K. Yu, M.W. McKittrick, C.W. Jones, Organometallics 23 (2004) 4089.
[80] H. Yoshitake, T. Yokoi, T. Tatsumi, Chem. Mater. 14 (2002) 4603.
[81] G. Engelhardt, D. Michel, High Resolution Solid-State NMR of Silicates and Zeolites, Wiley, New York, 1988.
[82] D.W. Sindorf, G.E. Maciel, J. Am. Chem. Soc. 105 (1983) 3767.
[83] G. Calleja, R. van Grieken, R. Garcia, J.A. Melero, J. Iglesias, J. Mol. Catal. A 182 (2002) 215.
[84] R. Anwander, H.W. Gorlitzer, G. Gerstberger, C. Palm, O. Runte, M. Spiegler, J. Chem. Soc. Dalton Trans. (1999) 3611.
[85] M.C. Capel-Sanchez, J.M. Campos-Martin, J.L.G. Fierro, J. Catal. 217 (2003) 195.
[86] E.P. Reddy, L. Davydov, P.G. Smirniotis, J. Phys. Chem. B 106 (2002) 3394.
[87] J. Tian, S.T. Wang, Y.D. Feng, J.M. Li, S. Collins, J. Mol. Catal. A 144 (1999) 137.
[88] J.H.Z. dos Santos, H.T. Ban, T. Teranishi, T. Uozumi, T. Sano, K. Soga, J. Mol. Catal. A 158 (2000) 541.
[89] X. Cheng, O.W. Loftus, P.A. Deck, J. Mol. Catal. A 212 (2004) 121.
[90] X.M. Yang, C.L. Stern, T.J. Marks, J. Am. Chem. Soc. 116 (1994) 10015.
[91] J.A. Ewen, M.J. Elder, US patent 5,561,092, 1996.
[92] E.Y.X. Chen, T.J. Marks, Chem. Rev. 100 (2000) 1391.
[93] Y.X. Chen, C.L. Stern, S.T. Yang, T.J. Marks, J. Am. Chem. Soc. 118 (1996) 12451.
[94] M. Mohammed, M. Nele, A. Al-Humydi, S.X. Xin, R.A. Stapleton, S. Collins, J. Am. Chem. Soc. 125 (2003) 7930.